VOL. 10, NO. 9, MAY 2015 ISSN 1819-6608
ARPN Journal of Engineering and Applied Sciences

www.arpnjournals.com

PERFORMANCE ASSESSMENT OF DIRECT AND INDIRECT CURRENT CONTROL STRATEGIES FOR SHUNT ACTIVE POWER FILTER

A. Sakthivel[1], P.Vijayakumar[2] and A.Senthilkumar[1]
[1]Department of Electrical and Electronics Engineering, Dr. Mahalingam College of Engineering and Technology, Pollachi, India
[2]Department of Electrical and Electronics Engineering, Karpagam College of Engineering, Coimbatore, India
E-Mail: ersakthi@yahoo.com

ABSTRACT

This paper compares Direct Current Control Technique (DCCT) and Indirect Current Control Technique (ICCT) for the control of Shunt Active Power Filter (SAPF). A current controlled voltage source inverter is used as SAPF and three-phase diode bridge rectifier with RL load is considered as Non-Linear Load (NLL). Dynamic response analysis of both techniques of current control is compared. Based on experimental results, it is evident that ICCT becomes simpler, requires less hardware and offers better performance.

Keywords: shunt active power filter, direct current control, indirect current control, dynamic response of controller, harmonic mitigation.

1. INTRODUCTION

Power converters are mainly utilized in domestic as well as industry applications for the control and conversion of electric power. The modern power electronic loads behave as NLL drawing sizable amount of harmonics from the utility mains. Their contributions to increased harmonic pollutions in utility system is of growing interest, and are responsible for various power quality issues, led to application of standard viz. IEEE 519-1992 [1-3]. The harmonic currents can interact adversely with a wide range of power system equipments causing additional losses, overheating, overloading, interference with telecommunication networks and leads to erroneous readings in watt-hour and demand meters [4, 5].

Parallel passive filter consists of inductors, capacitors and damping resistors has been used for harmonic mitigation. The increased severity of power quality disturbances and problems associated with the passive filters viz. large size and weight, higher cost, fixed compensation, and resonance problems with loads and networks have demanded the focus on power electronic based APFs. These are researched and developed as a viable alternative over the conventional practices to solve power quality problems. The SAPF can compensate harmonics and reactive power requirement of the NLL effectively [6, 7]. The Voltage Source Inverter (VSI) based SAPF is preferred choice by the utilities due to its increased efficiency compared to current source inverter based SAPF [8, 9].

The performance of SAPF is mainly on the selected reference extraction scheme. The reference signal that has to be processed by the PI controller is the main component, which ensures the proper operation of SAPF. Several methods are available for extracting the reference switching current for the APF [10]. ICCT based PI control algorithm is discussed in [11-13]. Misra et.al investigated the performance of SAPF employing bacteria foraging technique with Integral Time Square Error (ITSE) cost function. Sakthivel et.al investigated dynamic response analysis of SAPF using Ant Colony Optimization (ACO) technique also studied on various choice of cost function considering dynamic performance criterion viz. Integral Square Error (ISE), ITSE, Integral Absolute Error (IAE) and Integral Time Absolute Error (ITAE).

The proposed work aims to evaluate the performance of SAPF based on DCCT and ICCT based current control strategies for the control of shunt active power filter. The rest of the paper is organized as follows. Section 2 presents reference current extraction methodology and DCCT and ICCT strategies. ACO tuning approach to SAPF briefed in Section 3. Section 4 describes the test system followed by simulation results presented in Section 5. The conclusions are drawn in Section 6.

2. REFERENCE CURRENT EXTRACTION STRATEGY

The utility mains current is distortion free and is in phase with mains voltage once the SAPF is injecting the harmonic currents to PCC. The Figure-1 shows the compensation principle of three-phase SAPF.

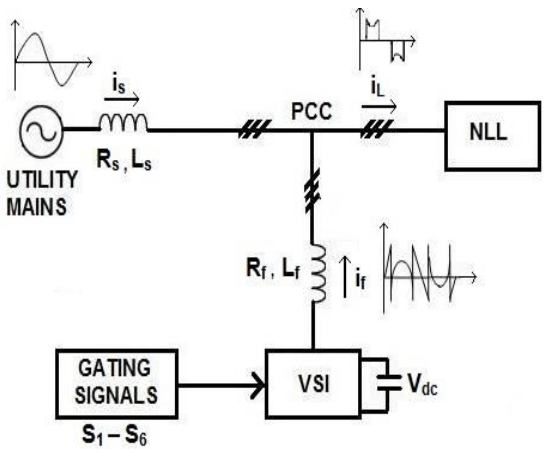

Figure-1. Compensation principle of SAPF.

The SAPF is controlled to inject the compensating current i_f in orderto make the supply mains current harmonics free irrespective of the load characteristics. Initially, the shape of the source current and load current aresame. Once the SAPF is connected at PCC the shape of source current would become sinusoidal, hence harmonics free.

From Figure-1, the instantaneous current at PCC is given by equation (1),

$$i_s(t) = i_L(t) - i_f(t) \quad (1)$$

The utility mains voltage is as given in equation (2),

$$v_s(t) = V_m \sin\omega t \quad (2)$$

NLL will draw current in a non-sinusoidal shape when it is connected to utility mains. This implies that load current consists of more than one frequency component, which can be expressed as in equation (3).

$$i_L(t) = \sum_{n=1}^{\infty} I_n \sin(n\omega t + \Phi_n)$$

$$i_L(t) = I_1 \sin(\omega t + \Phi_1) + \sum_{n=2}^{\infty} I_n \sin(n\omega t + \Phi_n) \quad (3)$$

The instantaneous load power then can be given in equation (4),

$$p_L(t) = v_s(t) * i_L(t)$$

$$= V_m I_1 \sin^2\omega t * \cos\Phi_1 + V_m I_1 \sin\omega t * \cos\omega t * \sin\Phi_1 + V_m \sin\omega t * \sum_{n=2}^{\infty} I_n \sin(n\omega t + \Phi_n) \quad (4)$$

$$p_L(t) = p_f(t) + p_r(t) + p_h(t) \quad (5)$$

It is seen from equation (4) and (5), fundamental power (6) drawn by the load is given by,

$$p_f(t) = V_m I_1 \sin^2\omega t * \cos\Phi_1 = v_s(t) * i_s(t) \quad (6)$$

From equation (6), the source current (7) supplied by the source, after compensation is given by,

$$i_s(t) = \frac{p_f(t)}{v_s(t)} = I_1 \cos\Phi_1 * \sin\omega t = I_{sm} \sin\omega t \quad (7)$$

where $I_{sm} = I_1 \cos\Phi_1$

Also there are some switching losses involved in the pulse width modulated VSI inverter. Thus, the utility mains should supply a small overhead for the capacitor leaking and inverter switching losses in addition to the real power demand of the load. Hence, the total peak current supplied by the utility mains is expressed as in equation (8).

$$I_{sp} = I_{sm} + I_{sL} \quad (8)$$

If, the SAPF is supposed to provide the total reactive and harmonic power (i.e. the equal and opposite amount of reactive and harmonic current), then $i_s(t)$ will be in phase with the utility mains voltage and non-distorted. Hence $i_s(t)$ consists of only fundamental component of mains supply current. The compensation current ($i_f(t)$) supplied by the SAPF is written as in equation (9).

$$i_f(t) = i_L(t) - i_s(t) \quad (9)$$

For the compensation of reactive and harmonic power, it is essential to calculate$i_s(t)$fundamental component of load current, which is subtracted from the load current. Hence, the filter current consists of harmonic components, which will be injected by SAPF at PCC if the filter is connected to the supply system. The three phase mains current after compensation is given as in equation (10).

$$\left.\begin{aligned} i^*_{sa} &= I_{sp} \sin(\omega t) \\ i^*_{sb} &= I_{sp} \sin(\omega t - 120) \\ i^*_{sc} &= I_{sp} \sin(\omega t - 240) \end{aligned}\right\} \quad (10)$$

I_{sp} – Peak value of the supply current

From equation (10), the shape of mains current waveform and its phase is known and only the mains peak current (I_{sp}) is to be calculated. I_{sp} can be calculated by regulating DC side capacitor voltage (V_{dc}) of PWM inverter. The $V_{dc}$is compared with reference value and the error is processed using PI controller. The response of the PI controller is considered as the peak value of utility mains current and the reference currents are calculated by simply multiplying this peak value with the unit sine signal in phase with the utility mains voltages. Figure-2 shows the configuration of three - phase SAPF. The modified Space Vector PulseWidth Modulation (SVPWM) current control scheme [14] is utilized in SAPF to generate the switching pulses of VSI.

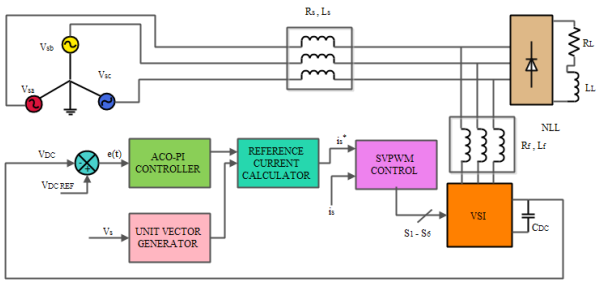

Figure-2. Configuration of Three - Phase SAPF.

A. Direct current control technique

Direct current control strategy is shown in Figure-3. It is intended that utility mains should supply fundamental active power to NLL and losses in the system. APF should supply the anti-harmonics of the load

at PCC. Thus the three-phase supply currents is sinusoidal and in phase with the utility mains voltages.

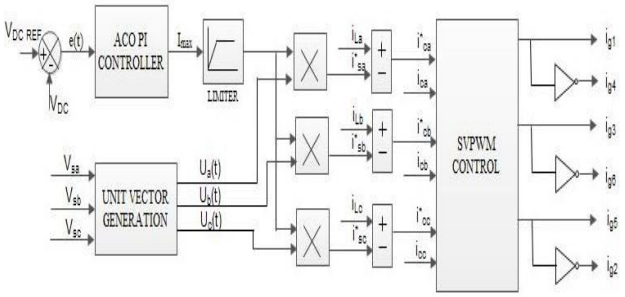

Figure-3. SAPF control algorithm with DCCT.

It is important to supply an additional active power to meet the losses in the SAPF system and to regulate the DC bus voltage of the SAPF. The DC side capacitor serves two important purposes such as it maintains a V_{dc} with a small ripple in steady state and it serves as an energy storage element to supply the real power difference between load and source during the transient period. In the steady state the real power supplied by the source should be equal to the real power demand of the load plus a small power to compensate for the losses in the APF. Thus V_{dc}can be maintained at a reference value and regulation of DC voltage ensures an effective control at the input side of the SAPF. Since the regulation of V_{dc} imparts a proper current control of the SAPF, the control scheme of the SAPF works with the DC bus voltage as a feedback signal in both DCCT and ICCT of current control. In this control strategy, reference $V_{dc}$is compared with actual $V_{dc.}$ The error voltage is processed using PI controller and the output of the controller is considered as peak reference supply current as shown in (8). The reference supply current is subtracted from load current, yields the reference filter current, which in turn compared with actual filter current. SVPWM technique is used to generate gating signals of VSI based SAPF.

B. Indirect current control technique

Indirect current control strategy is shown in Fig.4. In this control strategy, reference V_{dc} is compared with actual $V_{dc.}$ The error voltage is processed using PI controller and the output of the controller is considered as peak reference supply current as shown in (8). The rms value of reference supply current is compared with actual supply current and SVPWM technique is used to generate gating signals of VSI based SAPF.

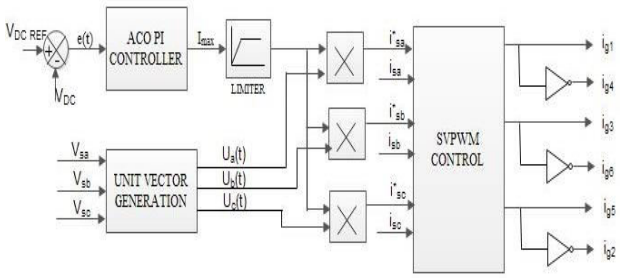

Figure-4. SAPF control algorithm with ICCT.

3. ACO TUNING APPROACH TO SAPF

The foraging behavior of ants is the main source of inspiration for the development of ACO. Marco Dorigo presented the ACO algorithm in [15] and carried out further investigations [16-17]. The feature of ant colony algorithm is that it employs positive feedback, distributed computation, and constructive greedy heuristic. Positive feedback accounts for fast discovery of good solutions, distributed computation avoids premature convergence and greedy heuristic helps to find acceptable solutions in the early stages of the search process [18]. ACO is an evolutionary meta-heuristic algorithm based on a graph representation. The main idea of ACO is to model the problem as the search for a minimum cost path in a graph. In ACO technique, artificial ants mimic the foraging behavior of their biological counterparts in finding the shortest path to the food source. Ant deposits pheromone while crawling, the ant following shortest path collects more amount of pheromone per time unit and, in turn, more number of ant selects the shortest path due to positive feedback. All ants move nearly at the same speed and deposit a pheromone trail at around the same rate. This makes the increase of pheromone trail rapidly on the shortest side.

A. ACO-PI tuning approach to SAPF

ACO algorithm used for tuning PID and nonlinear PID controllers perform better [19]. The ACO approach for the tuning of PI controller used in SAPF is shown in Figure-5.

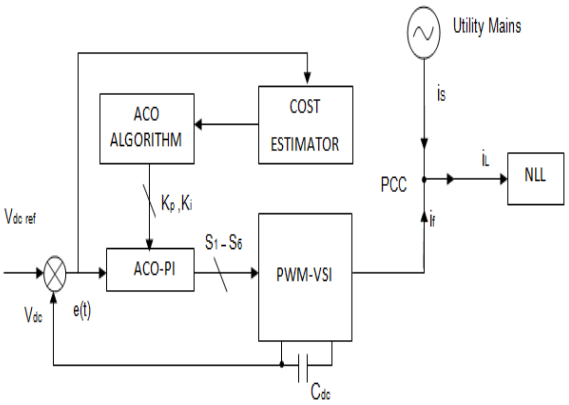

Figure-5. ACO tuning approach for SAPF PI controller.

The cost function is estimated based on e(t) and supplied to the ACO algorithm to find the optimal search.

Table-1. SAPF (5KVA) system parameters.

V_s - AC supply voltage	**100 V** (peak)
R_s - Source resistance	0.1 Ω
L_s – Source inductance	0.15 mH
V_{dco} -Steady state operating point of V_{dc}	220 V
C_{dc}- DC side capacitor	2000 µF
I_{fo} Steady state operating point of I_f	23.57 A
L_f - Filter inductance	0.66 mH
R_f - Filter resistance	0.1 Ω
R_L - Load resistance	6.7 Ω
L_L - Load inductance	20 mH
$V_{dc\ ref}$ - Reference DC link voltage	220 V

4. SAPF SYSTEM PARAMETERS

For a 5-kVA APF, the system parameters are presented in Table-1 [12-13]. The values of conventional PI controller proportional gain and integral gain are selected as 0.57 and 10.3 respectively [12]. Author presented the ACO algorithm for obtaining the proportional gain (K_P) and integral gain (K_i) values of PI controller used in SAPF in [13]. In this paper, the optimized gain values [13] obtained for different cost functions is utilized to compare the performance of DCCT and ICCT of SAPF with conventional values.

5. EXPERIMENTAL RESULTS

As per the parameters given in Table-1, the Simulink model of SAPF was developed using MATLAB SimPowerSystem toolbox. The K_p and K_i gain values are obtained for different cost functions, for the proposed ACO approach and conventional design are listed in Table-2. The performance of the proposed approach is evaluated in terms of its dynamic performance analysis as detailed below.

A. Dynamic performance of SAPF

Three-phase input source voltages are considered to be balanced and sinusoidal. The diode bridge rectifier non-linear load is considered for load compensation. The Total Harmonic Distortion (THD) before SAPF is connected to PCC is 28.01%. The performances of SAPF with the ACO-PI controller and conventional PI controller have been analyzed using DCCT and ICCT based control strategies for the following two different cases.

Case-1. Switch-on response: The SAPF is switched on at t=50ms. The performance of DC capacitor voltage regulation with conventional PI controller and ACO-PI controller for various objective functions are depicted in Figure-6. The performance indices for SAPF considered are V_{dc} settling time (V_{dc}_T_s), Percentage peak overshoot (%M_p), ISE, ITSE, IAE, ITAE and %THD and the values of the performance indices for switch-on response are listed in Table-2.

For comparing the performance measures shown in Table-2, the values of K_p and K_i for the ACO based PI controller are kept at 0.964 and 298.84, respectively. It is seen from Figure-6 that the ACO PI controller with ISE as cost function offers better convergence of capacitor voltage compared to all other cost functions. The supply voltage (V_{sa}), supply current (I_{sa}), loadcurrent (I_{La}), filter current (I_{fa}), and V_{dc} related to phase-a of conventional PI controller and ACOPI controller are shown in Figure-7 and Figure-8 respectively. The source current of ACO PI becomes purely sinusoidal within one cycle and capacitor voltage settles at 28.5ms compared to conventional controller, which takes310ms.In all the cases, %THD is within the limit of IEEE 519-1992 standard. Thus, for further discussions, we use ACO PI controller with ISE objective function only.

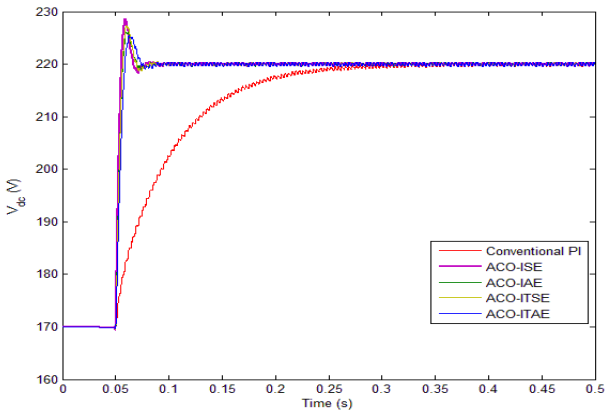

Figure-6. V_{dc} during switch-on response for conventional PI and ACOPI using ICCT.

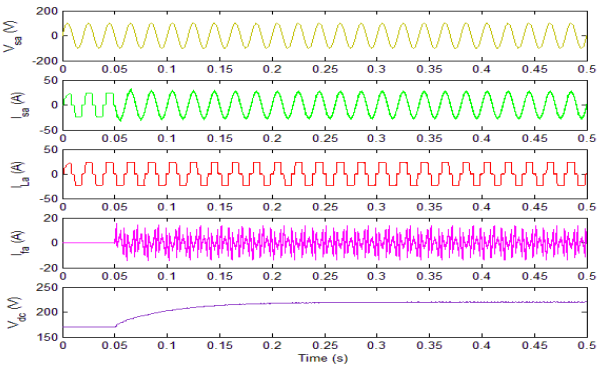

Figure-7. V_{sa}, I_{sa}, I_{La}, I_{fa} and V_{dc} of conventional PI controller using ICCT.

Case-2. Transient response: In order to perform the transient response analysis, the load resistance is increased from 6.7 Ω to 10 Ω at t = 0.3 s (shown in Figure-9).

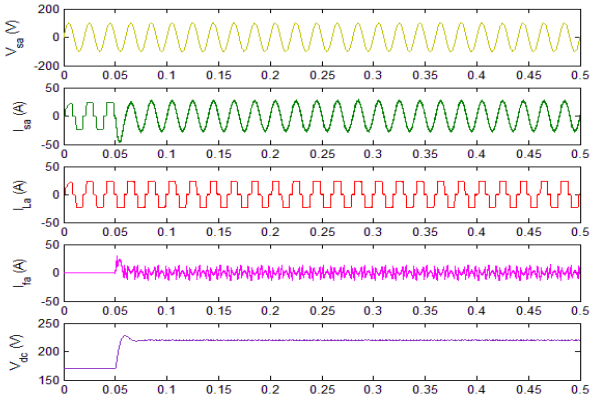

Figure-8. V_{sa}, I_{sa}, I_{La}, I_{fa} and V_{dc} of ACOPI controller using ICCT.

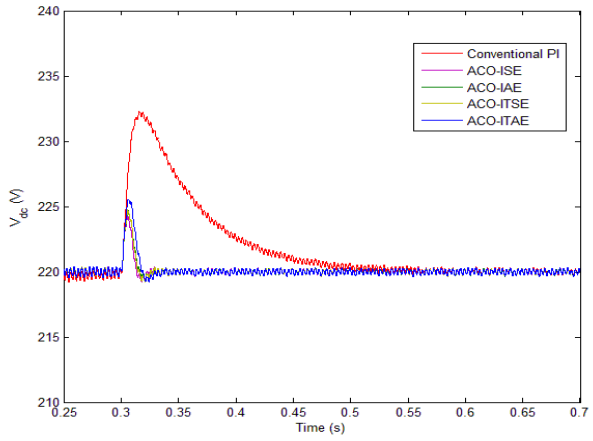

Figure-9. V_{dc} for varying R_L (6.7 Ω to 10 Ω) using ICCT.

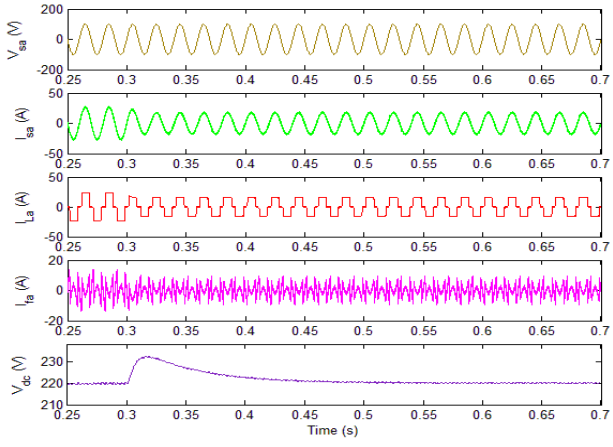

Figure-10. V_{sa}, I_{sa}, I_{La}, I_{fa} and V_{dc} of conventional PI controller for varying R_L (6.7 Ω to 10 Ω) with ICCT.

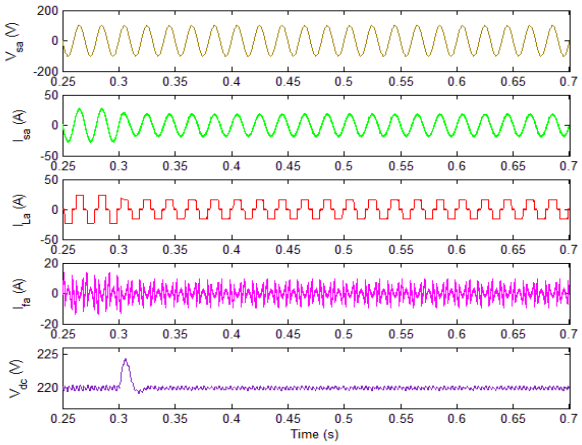

Figure-11. V_{sa}, I_{sa}, I_{La}, I_{fa} and V_{dc} of ACOPI controller for varying R_L(6.7 Ω to 10 Ω) with ICCT.

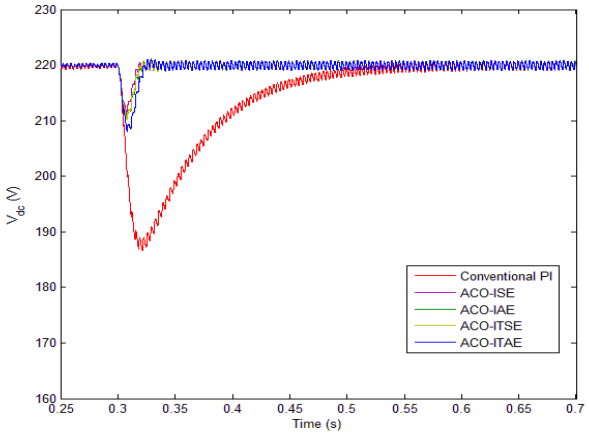

Figure-12. V_{dc} for varying R_L (6.7 Ω to 3.4 Ω) using ICCT.

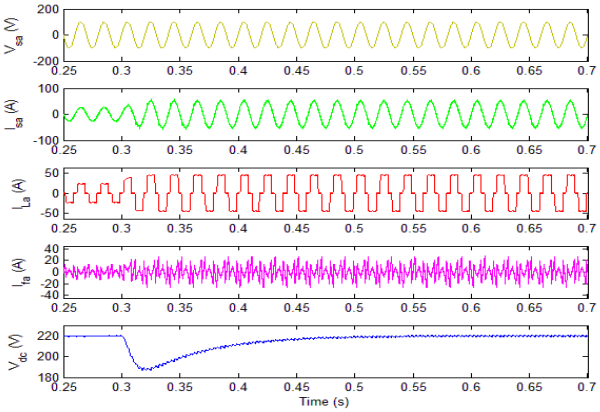

Figure-13. V_{sa}, I_{sa}, I_{La}, I_{fa} and V_{dc} of conventional PI controller for varying R_L (6.7 Ω to 3.4 Ω) with ICCT.

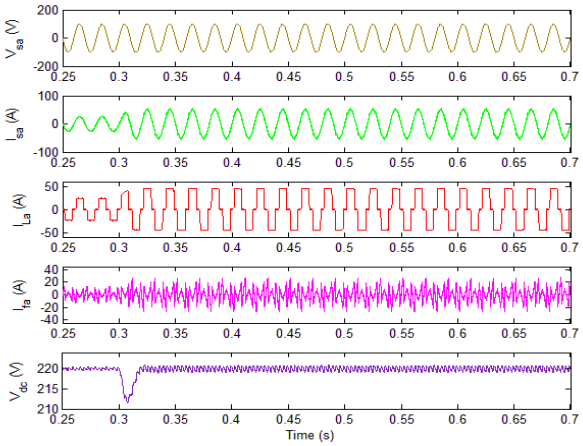

Figure-14. V_{sa}, I_{sa}, I_{La}, I_{fa} and V_{dc} of ACOPI Controller for varying R_L(6.7 Ω to 3.4 Ω) with ICCT.

The response of DC bus voltage during load change for the conventional PI and ACO PI controller with different cost functions are depicted in Figure-9. The supply voltage (V_{sa}), supply current (I_{sa}), load current (I_{La}), filter current (I_{fa}), and V_{dc} related to phase-a of conventional PI controller and ACO PI ISE controller are shown in Figure-10 and Figure-11 respectively. To evaluate the dynamic response for decreasing load, we vary the R_L from 6.7 Ω to 3.4 Ω at t=30ms. The DC voltage response during load change for the conventional PI and ACO PI controllers are shown in Figure-12. The V_{sa}, I_{sa}, I_{La}, I_{fa}, and V_{dc} related to phase-a of conventional PI controller and ACO PI ISE controller are shown in Figure-13 and Figure-14 respectively. Performance analyses for the two different cases using ICCT were shown in Figure-6 to Figure-14. SAPF were analyzed using DCCT based control strategy and the results for both control strategies are presented in Table-2 and Table-3. For ACO PI controllers the source currents become sinusoidal within a cycle. In conventional PI controller, dip in V_{dc} is larger and takes more cycles to settle down, % THD in source current settles to nominal value within 3 - 4 cycles. Source current THD spectrum is shown in Figure-15. The ACO PI controller show more than ten times reduction in settling time for increasing load R_L and more than fifteen times reduction in settling time for decreasing load compared to the conventional PI controller. This is due to the use of statistical parameters as performance criterion for optimization in the proposed ACO PI approach. Also note that, from Table-3 the ACO approach show better reduction in %rise/dip in DC capacitor voltage compared to conventional design. This offers rapid reduction in settling time of the ACO approach.

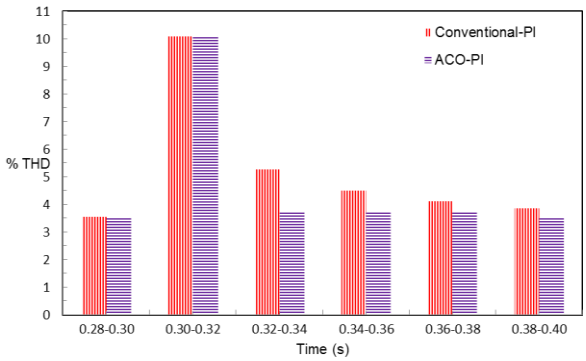

Figure-15. Source current Harmonic Spectrum for DCCT and ICCT.

Comparing the experimental results discussed from Table-2, Table-3 and Table-4, dynamic response of both DCCT and ICCT based strategies are similar. ICCT requires only three current sensors and becomes simpler, where DCCT used six current sensors.

Table-2. Performance analysis of SAPF for conventional pi and ACO pi controllers with DCCT and ICCT.

Controller type / Parameters	Conventional PI	ACO-PI : ISE	ACO-PI: ITSE	ACO-PI: IAE	ACO-PI: ITAE
Kp	0.57	0.964	0.912	0.962	0.813
Ki	10.3	298.84	247.92	238.77	170.78
Vdc_Ts (ms)	310	28.5	32	32	38.5
% Mp	0	3.96	3.32	2.77	2.47
% THD	3.88	3.74	3.72	3.72	3.67
ISE	55.36	4.781	5.172	4.969	6.287
ITSE	4.188	0.2538	0.2538	0.2631	0.3337
IAE	2.412	0.2848	0.2956	0.2848	0.3273
ITAE	0.2532	0.0365	0.0371	0.0364	0.0363

Table-3.

Comparative transient analysis of SAPF for conventional Pi and ACO Pi controllers with DCCT and ICCT variations in load	Settling Time (ms)		% rise/dip in dc capacitor voltage		ISE	
	Conventional PI	ACOPI	Conventional PI	ACOPI	Conventional PI	ACO PI
R_L increased from 6.7Ω to 10 Ω	≈260	≈25	5.6	1.97	56.6	3.539
R_L decreased from 6.7Ω to 3.4 Ω	≈300	≈20	15.16	3.92	96.35	4.018

Table-4. DCCT vs ICCT hardware components.

Current control technique	Voltage sensor	Current sensors
DCCT	4	6
ICCT	4	3

6. CONCLUSIONS

Direct and indirect current control strategies were discussed in detail. Capability of DCCT and ICCT were investigated for two different dynamic conditions. Comparing the results of both techniques, the dynamic response of both current control strategies in terms of DC bus voltage settling time, %rise/dip in DC capacitor voltage and total harmonic distortion becomes similar for both conventional and optimized controller gain values. Indirect current control technique is simpler, requires less hardware and offers better performance.

REFERENCES

[1] H. Akagi, Y. Kanazawa, and A. Nabae, "Instantaneous reactive power compensator comprising switching devices without energy storage components," IEEE Transactions on Industry Applicaions, vol. IA-20, No.3, pp. 625–630, May/June 1984.

[2] H. Akagi, E. H. Watanabe and M. Aredes, Instantaneous power theory and applications to power conditioning, IEEE Press Series On Power Engineering; John Wiley and Sons, New Jersey, 2007.

[3] S. K. Jain, P. Agarwal and H.O. Gupta, "Design simulation and experimental investigations on a shunt active power filter for harmonics and reactive power compensation" Electric Power Components and Systems, vol. 31(7), pp. 671–692, 2003.

[4] A. A. Mahmoud and R. E. Owen, "Power system harmonics: An overview", IEEE Transactions on Power Apparatus and Systems, vol. 8, pp. 2455–2460, 1983.

[5] Institute of Electrical and Electronics Engineers, "Recommended Practices and Requirements for Harmonic Control in Electrical Power Systems", 1992.

[6] H. Akagi, "New trends in active filters for power quality conditioning," IEEE Transactions on Industry Applications, vol. 32, No.6, pp. 1312–1322, November/December 1996.

[7] S. K. Jain, P. Agarwal and H.O. Gupta "A control algorithm for compensation of customer-generated harmonics and reactive power," IEEE Transactions on Power Delivery, vol. 19, No.1, pp. 357–366, January 2004.

[8] W. M. Grady, M. J. Samotyj, A. H. Noyola, "Survey of active power line conditioning methodologies", IEEE Transactions on Power Delivery, vol. 5, No.3, pp. 1536-1542, July 1990.

[9] M. Routimo, M. Salo, H. Tuusa, "Comparison of voltage source and current source shunt active power filters", IEEE Transaction on Power Electronics, vol. 22, No. 2 pp. 636-643, March 2007.

[10] Bhim Singh, Kamal Al-Haddad, Ambrish Chandra, "A review of active filters for power quality improvement", IEEE Transactions on Industrial Electronics, vol. 46, No. 5, pp.960-971, October 1999.

[11] S. Jain, P. Agarwal, H. O. Gupta, "Design simulation and experimental investigations on a shunt active power filter for harmonics and reactive power compensation", Electric Power Components and System, vol. 32, No. 7, pp. 671–692, 2003.

[12] S. Mishra, C. N. Bhende, "Bacterial foraging technique-based optimized active power filter for load compensation", IEEE Transactions on Power Delivery, vol. 22, No.1, pp. 457-464, 2007.

[13] Sakthivel Aruchamy, Vijayakumar P, Senthilkumar A, "Design of Ant Colony Optimized Shunt Active

Power Filter for Load Compensation", International Review of Electrical Engineering, Vol. 9, No.4, 725-734, 2014.

[14] Microsemi User Guide, Space Vector Pulse Width Modulation Hardware Implementation, 2014.

[15] M. Dorigo, Optimization, learning and natural algorithms (in Italian). Ph.D. dissertation, Dipartimento di Elettronica, Politecnico di Milano, Italy, 1992.

[16] M. Dorigo, V. Maniezzo, and A. Colorni, Ant System: Optimization by a colony of cooperating agents. IEEE Transactions on Systems, Man, and Cybernetics-Part B, 1996; 26(1): 29-41.

[17] Marco Dorigo, Mauro Birattari, and Thomas Stutzle. Ant Colony Optimization. IEEE Computational Intelligence Magazine, 2006; 28-39.

[18] Marco Dorigo, Thomas Stutzle. Ant Colony Optimization. England: MIT Press, 2004.

[19] Muhammet Ünal, Ayça AK, Vedat Topuz, and Hasan Erdal. Optimization of PID Controllers Using Ant Colony and Genetic Algorithms.Springer-Verlag Berlin Heidelberg, 2013.